

<https://doi.org/10.1038/s40494-025-01631-z>

Reconstruction of the paleoenvironmental context of Holocene human behavior at the Fenghuangzui site in the Nanyang Basin, Middle Yangtze River, China

Check for updates

Aipeng Guo¹, Longjiang Mao²✉, ChenChen Li¹ & Duowen Mo³

Geomorphological research at archaeological sites reveals that environmental factors, such as geomorphology and hydrology, play a crucial role in understanding changes in site layout and cultural processes. However, due to the lack of reliable chronologies, there is limited understanding of environmental factors in relation to archaeological site. This study focuses on the sedimentary records from the southern moat of the Fenghuangzui (FHZ) site, a representative site in the middle Yangtze River region, integrating a chronological framework and climate proxies such as elemental geochemistry. It reconstructs the evolution of the regional sedimentary environment and the hydrogeomorphology during the mid-late Holocene at the FHZ site, elucidating its interplay with human activities. Key findings include: (1) From 5.6–4.5 ka BP, elevated chemical index of alteration (CIA), Rb/Sr, and Mn/Ti values indicate a warm and humid climate. The Qujialing culture unified the middle Yangtze River and established regional central settlements such as Shijiahe site, and then expanded to the north. The FHZ site was built in the Nanyang Basin at this time to prevent the invasion of northern culture. (2) During 4.5–4 ka BP, decreased CIA and Rb/Sr values alongside rising secondary aluminum factor (Saf) and dealkalization coefficient (Bc) values signify reduced weathering and a transition to cooler, drier conditions. A flood event of 4–3.9 ka BP caused the moat of the FHZ site to lose its defensive function. (3) During 4–2.7 ka BP, declining CIA and Rb/Sr values with slight increases in Saf and Bc suggest ongoing dry and cool environmental conditions. The FHZ site was abandoned at the end of the Meishan culture. (4) Between 2.7–1.6 ka BP, rising CIA and Rb/Sr values indicate a return to warmer and more humid conditions. The FHZ site was built to expand the influence of Qujialing culture and protect the Shijiahe settlement. Taking into account the location of the water system and farming area, the south-facing direction was chosen. In general, our findings suggest that changes in regional hydrology in the context of climate change can trigger upheaval and even collapse of prehistoric societies.

Over the past approximately 20 ka, the global climate has undergone significant changes, marked by an overall warming trend from the Last Glacial Maximum (LGM) to the Holocene thermal maximum, followed by a general cooling trend^{1–3}. During this interval, the dynamic interaction between climatic fluctuations and environmental changes influenced

diverse civilizations and cultural landscapes^{4,5}. Recent studies frequently underscore the synchronicity between climatic events and significant cultural shifts. This encompasses the influence of natural elements, such as climatic fluctuations, precipitation patterns, and geomorphic evolution on the settlement patterns, survival strategies, and sociocultural practices

¹Institute of Science and Technology History and Meteorological Civilization, Nanjing University of Information Science and Technology, Nanjing, 210044, China.

²School of Marine Science, Nanjing University of Information Science and Technology, Nanjing, 210044, China. ³College of Urban and Environmental Sciences, Peking University, Beijing, 100871, China. ✉e-mail: mjl1214@163.com

within human communities^{6–9}. For example, the 4.2 ka BP event in the mid-late Holocene had varying degrees of impact on early civilizations¹⁰. During this period, the collapse of agrarian societies and large human migration events occurred in the Nile Valley and eastern China due to climatic droughts, among others^{11,12}. The dwindling of river flooding spurred intensive agriculture in the Harappan civilization, yet the subsequent drying of monsoonal rivers led to a gradual migration towards the northern, more humid regions¹³. Thus, it is imperative to fully consider the roles of climatic and environmental factors to comprehensively understand the process of human civilization.

The generally warm climate of the Holocene provided favorable conditions for the development of agriculture during the Neolithic period^{14,15}. During this period, regions including the Nile Valley in Egypt¹⁶, the Yellow River basin^{17,18}, and the Yangtze River basin in China¹⁹ experienced the Holocene Climate Optimum (HCO). The HCO fostered abundant water resources and fertile soils, facilitating the emergence of agriculture and prehistoric cities^{20,21}. The middle Yangtze River region is influenced by the East Asian monsoon and has complex hydrological features, making them one of the origins of rice agriculture²². Between 6.5–5.3 ka BP, regional center settlements such as Chengtoushan site, with structures like walls, water fields, and water conservancy systems, appeared in the Dongting Lake Basin under favorable hydrological conditions. These settlements exhibited clear social hierarchical differentiation¹⁹. From 5.3–3.9 ka BP, many large and interconnected settlements emerged in the middle Yangtze River region. During this period, 20 regional center settlements were established and continuously used²³. However, precipitation alone could not meet the water demands of large regional center settlements, necessitating the consideration of natural water systems in site selection and usage. Ring trenches, as important water management facilities, provided conveniences for flood control, drainage, transportation, military defense, and agricultural production²⁴. Therefore, the establishment and use of regional center settlements were closely linked to the geomorphology and hydrology of the regional environment. The climatic deterioration around 4.2 ka BP may have led to the decline of the culture in the middle Yangtze River region, with many large settlements abandoned and gradually occupied by the northern Central Plains culture²⁵. Previous studies have extensively explored the environmental evolution and human activities in the middle Yangtze River, focusing on large environmental datasets from sedimentary records in the Jiangnan Plain²⁶ and Dongting Lake Plain²⁷, stalagmite records from Shanbao Cave in Shennongjia²⁸, and the distribution of Neolithic sites in relation to climatic change events^{19,25}, as well as the reasons for the mass decline and migration of the settlement sites²⁹. Despite the rich history of archaeological and paleoclimatic environmental studies in the middle Yangtze River, there remains a gap in studies that directly relate the regional environmental context to the development of center settlements.

The FHZ site, a Neolithic settlement, is located in the middle Yangtze River region at the southern edge of the Nanyang Basin. It is the largest and highest-grade central settlement site found so far in Nanyang Basin of Northwest Hubei. Recent research has shown that the construction of the city wall dates back to the Qujialing culture period, making it the highest known Qujialing culture site in terms of latitude. During the Shijiahe culture period, the moat of the FHZ site lost its defensive function and was used only for irrigation. The FHZ site was transformed from a regional central settlement to an ordinary settlement. After the Meishan culture, the site was completely abandoned³⁰. The moat outside the city wall is connected to the Paizihe River, forming a water conservancy system. The remains of the city wall and the river of the central settlements show that the construction of the central settlements had a close connection with the natural environment. After a number of archaeological excavations, related scholars have studied the function, structure and identification of plant remains of the site^{31,32}. Although environmental factors evidently influenced the establishment and development of the FHZ site, much remains unknown about how regional environmental changes specifically affected the use and eventual

abandonment of cities. Furthermore, more precise chronological data is needed to directly link paleoenvironmental change with human activities during specific periods.

This study collected sedimentary information from various cores in different landforms of the FHZ site and conducted a comprehensive comparative analysis using geochemical element records, grain size parameters, and archaeological records. The objectives of this paper are to: reconstruct the paleoclimate changes at the FHZ site², analyze the evolution of regional landforms and hydrology in the study area, and³ elucidate the relationship between climate fluctuations, hydrological dynamics, and the formation and decline of the FHZ site.

The study area is located in the southern part of the Nanyang Basin in the middle Yangtze River Valley, east of the Hanjiang River (Fig. 1a). The Nanyang Basin is bounded in the southeast by the Dabie Mountains, in the southeast by the Jiangnan Basin through the Suizhou Corridor, in the north by the Founiu Mountains, in the east by the Tongbai Mountains, in the west by the Qinling Mountains, and in the south by the remnants of the Daba Mountains. The edge of the basin is a hilly area with an altitude of 140–200 m, and there are gentle valley depressions between the hills. The main rivers in the area are the Tang River, the Bai River, the Tujia River, the Dan River, and the Han River, which is the largest tributary of the Yangtze River³³. The study area has a northern subtropical monsoon climate. It is characterized by simultaneous rain and heat, and four distinct seasons. The main body of the study area is located in Xiangyang City, where the average annual temperature is between 15–16 °C, except for the high mountains. The city is rich in heat resources and has a more obvious transitional nature, combining the characteristics of north and south climate. The city's annual precipitation ranges from 820–1100 mm, of which 400–450 mm are recorded in summer. Solar radiation is relatively abundant, with an annual average total sunshine duration of 1800–2100 h. The Nanyang Basin is located in the central China, between the Yangtze River and the Yellow River, and is a hub between the north and the south³³.

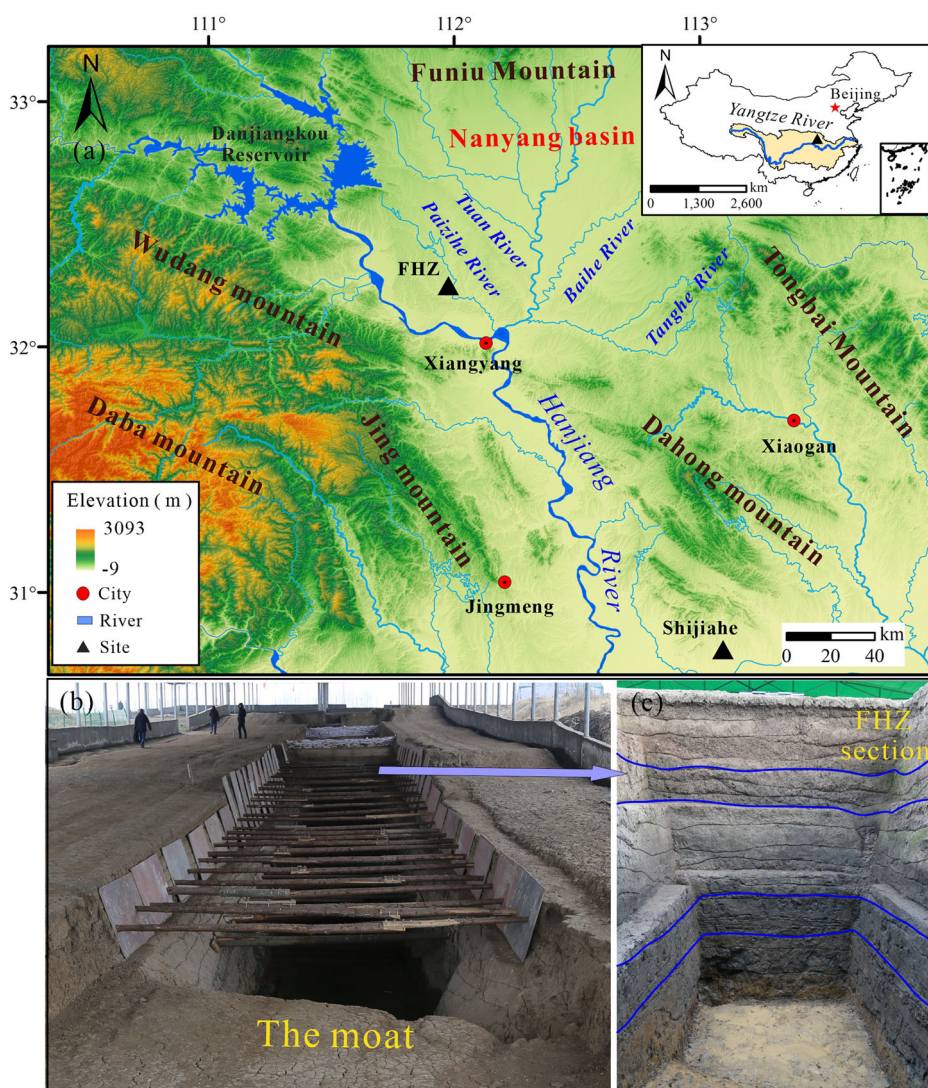
The FHZ site (111°59'20.39"E, 32°14'042.67"N, highest elevation 94 m) is located in Xiangyang City, Hubei Province. The site is located in the eastern plain of the Hanshui River, open and flat in the north, and connected to the Dahong Mountain in the south, with the geomorphological features transitioning from alluvial plains and hilly plains to hills. The FHZ site was built on an irregularly shaped terrace, and is bordered by the Paizi River in the east. The inner settlement of the site occupies an area of nearly 140,000 m², with a total area of about 500,000 m². The site is roughly square in plan, enclosed by walls and a moat. Based on the total area of the FHZ site, the architectural remains within the settlement, especially the high-grade architectural sites, and the excavated jade and turquoise ornaments, it can be inferred that the site had a high status and was the regional center of Northwest Hubei³⁰.

Materials and methods

Stratigraphy and sampling

Based on the terrain and archaeological records, we chose to collect samples from a trench located south of the moat at the FHZ site. This trench was excavated by the archaeological team of FHZ Site from Wuhan University and connects the southern moat to the city wall (Fig. 1b). The distance between the moat and the city wall is 3 meters, with a large amount of braised soil and cultural remains inside the wall. We chose to sample the section of the moat, which was 6.25 m. The profile is clearly stratified, and two periods of high water levels can be observed, and the bottom is a raw soil layer without human activity (Fig. 1c). The cultural layer is very thick, the internal accumulation of the moat can be divided into four periods: the historical period, the Meishan culture, the Shijiahe culture, and the Qujialing culture. It can be inferred from the pottery remains that the moat was used from the Qujialing Cultural period to the Ming and Qing dynasties. However, the use as well as the hydrological dynamics of each period varied greatly. The lithology of sediment cores was first observed in the field, and detailed lithological descriptions. The stratigraphic delineation is based on a combination of

Fig. 1 | Location, geomorphology, and stratigraphy of the FHZ site, Yangtze River basin. a Location of the FHZ site in the Yangtze River region, b the Southern Moat of the FHZ site. c the FHZ section, the area between the blue lines represents periods of high water levels.



observations of soil color, texture, structure, and inclusions. The profile is described according to Fig. 2.

Chronology

The optically stimulated luminescence (OSL) dating experiment was completed at the Shaanxi Key Laboratory of Earth Surface System and Environmental Carrying Capacity, NorthWest University, with a combined total of five samples. The experimental steps were as follows: (1) Prior to sample collection, the exposed portion of each sample was chipped in a laboratory darkroom to ensure accurate test results. Subsequently, the center portion of the sample was treated with a 30% solution of H₂O₂ and HCl to remove organic and carbonate material. (2) In order to obtain the quartz fractions required for dating, the medium-grained (45)63 μm mixed minerals were screened using the wet sieve method. Subsequently, the feldspar component of the medium-grained mixed minerals was removed by using 30% fluorosilicic acid, resulting in a pure quartz sample for subsequent equivalent dose measurements. (3) Equivalent dose measurements were performed using a Risø-TL/OSL DA-15 DASH light release meter. During the measurements, the excitation light source was blue light (470 ± 30 nm) and the photomultiplier tube was preceded by two filters of U-340. The measuring instrument was equipped with a radioactive β-source ⁹⁰Sr/⁹⁰Y and all artificial radioactive irradiations were performed on this instrument. The monolithic regenerative dose (SAR) method was used to obtain accurate equivalent dose data. Detailed dating results are shown in

Table 1. AMS ¹⁴C dating was conducted at Beta Analytic, USA. To mitigate the influence of organic contaminants, a standard acid-alkali-acid treatment along with solvent extraction was implemented before dating. The radiocarbon dates obtained in this study were calibrated using CALIB 8.2 and the IntCal20 calibration curve^{34,35}. Detailed dating results are shown in Table 2.

Geochemistry

Geochemical elemental analysis experiments were completed in the Provincial Key Laboratory of Anhui Normal University as follows: (1) The samples were air-dried. Based on the mass difference of the sample in the wet state and the dry state, the proportion of adsorbed water in the sample was determined, and the amount of adsorbed water was calculated. The samples with adsorbed water content greater than 1% were dried in an oven at 50–60 °C for 1 d. (2) The dried samples of not less than 5 g were grinded to 200 mesh and homogenized in agate mortar. Clean the container after each crushing operation to reduce the pollution of the residual sample to the subsequent sample. (3) Take the above grinding and mixing of powder samples 5–6 g into the plate mold with a diameter of 35 mm in a plastic cup, add 30 t pressure molding, pressing out the thickness of 2–4 mm disc. The discs were placed on an X-ray fluorescence spectrometer (XRF) for qualitative testing. The experimental instrument was a ZSX Primus IV X-ray fluorescence spectrometer (XRF) produced by Rigaku, Japan. The analytical process was monitored by National Geochemical Standard Sediment Samples (GSS1 and GSD9), and the analytical error was less than ±1%.

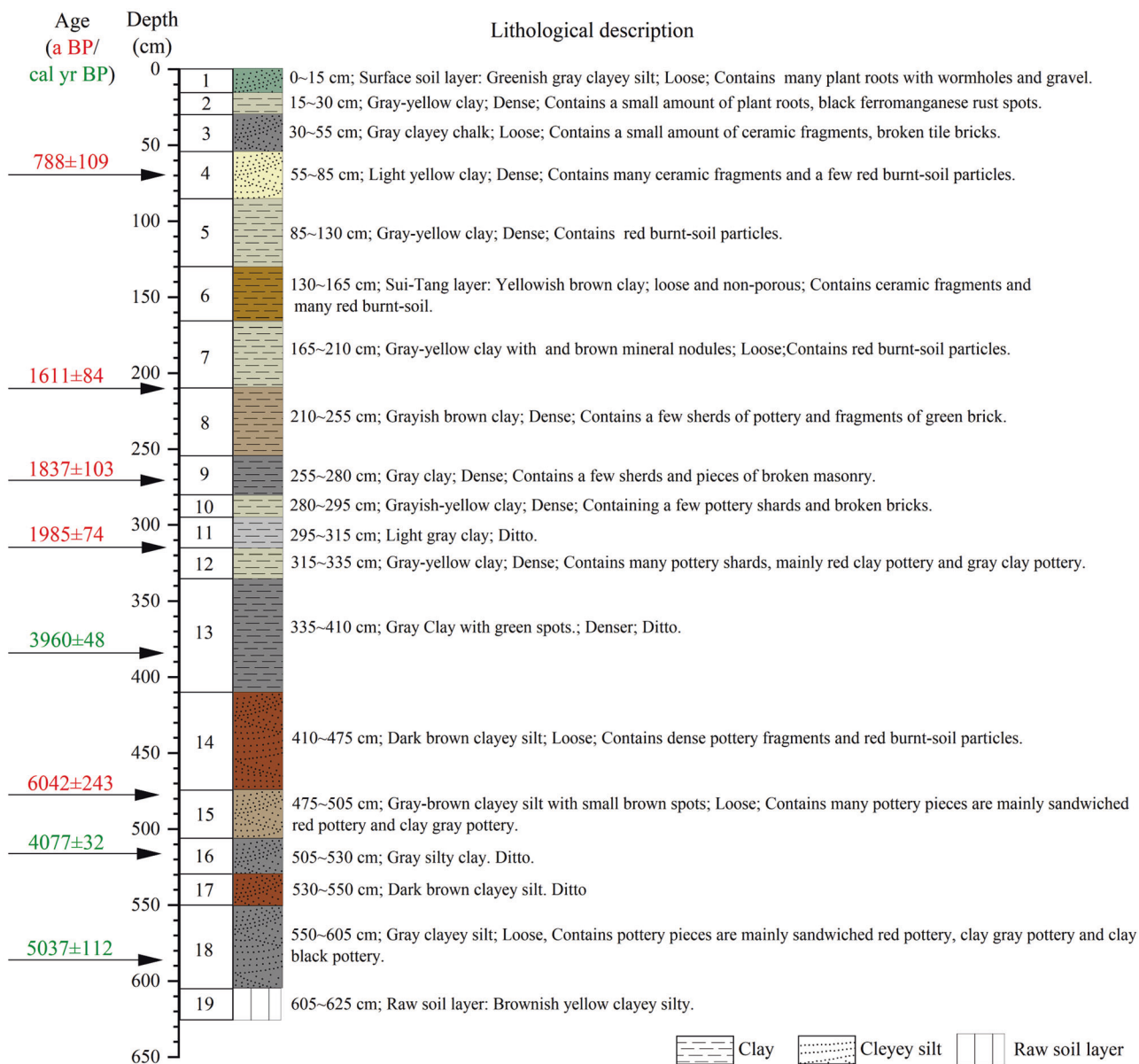


Fig. 2 | Lithologic description and chronological sampling from the FHZ section. Red text indicates optically stimulated luminescence ages, and green text indicates is the AMS ¹⁴C ages.

Table 1 | OSL dating results from FHZ section

OSL No.	Depth (cm)	U (mg/kg)	Th (mg/kg)	K (%)	Dose rate-MAM (Gy/ka)	Dose rate-CAM (Gy/ka)	Aliquots (n)	MAM-De (Gy)	Age (a BP)
01	70	1.98 ± 0.3	11.61 ± 0.7	1.82 ± 0.04	2.3 ± 0.31	2.65 ± 0.26	11	1.01 ± 0.09	788 ± 109
02	210	1.79 ± 0.3	10.38 ± 0.7	1.76 ± 0.04	4.38 ± 0.18	4.83 ± 0.28	20	2.48 ± 0.08	1611 ± 84
03	270	1.85 ± 0.3	11.25 ± 0.7	1.90 ± 0.04	5.32 ± 0.27	5.58 ± 0.16	32	10.51 ± 0.41	1837 ± 103
04	315	1.92 ± 0.3	11.28 ± 0.7	1.89 ± 0.04	5.74 ± 0.16	5.75 ± 0.12	23	21.28 ± 2.07	1985 ± 74
05	483	1.95 ± 0.3	12.15 ± 0.7	1.89 ± 0.04	17.67 ± 0.91	17.71 ± 0.46	19	19.73 ± 2.42	6042 ± 243

Table 2 | AMS ¹⁴C dating results of FHZ section⁶⁷

Laboratory No.	Depth (cm)	Cultural stage	AMS ¹⁴ C age (yr BP)	Cal radiocarbon age (2σ range, cal yr BP)	Weighted mean age (cal yr BP)
Beta-597333	382.5	Meishan culture	3640 ± 30	3849–3858 (0.011) 3870–4006 (0.8) 4032–4083 (0.189)	3960 ± 48
Beta-597334	517.5	Meishan culture	3740 ± 30	3984–4155 (0.948) 4204–4226 (0.052)	4077 ± 32
Beta-597335	585	Qujialing culture	4430 ± 30	4873–5060 (0.710) 5104–5132 (0.045) 5176–5276 (0.246)	5037 ± 120

Grain size

The particle size experiment was completed in the Marine Geology Teaching Laboratory of Nanjing University of Information Science and Technology. The experiment mainly includes two parts: sample pretreatment and instrumental measurement and analysis. The experimental steps are as follows: (1) Take 0.3–0.5 g of sample into a beaker, add 10 ml of H_2O_2 , shake well, heat and boil until no tiny bubbles. The purpose is to decompose the organic matter in the sample (such as humus and organic residues). (2) Continue to add 10 ml of HCL at 10% concentration to the beaker. The purpose of adding HCL is to remove carbonate minerals. (3) Add distilled water and leave it to stand, use a pipette to suck out the upper and middle clear liquid. Add 10 ml of $(NaPO_3)_6$ solution with 0.5% concentration, and oscillate in an ultrasonic cleaner for about 10 min to obtain a highly dispersed suspension, (4) Measure the particle size with a laser particle size analyzer. The Mastersizer 2000 laser particle size analyzer was used to analyze 350 sediment particle size samples. The measurement range of the instrument is 0.02–2000 μm , and the relative error of repeated measurements is less than 2%. The particle size parameters mean particle size (M_z), sorting coefficient (S_d), skewness (S_k), and kurtosis (K_u) were calculated using the GRADISTAT program.

Results

Sediment chronology

Five OSL dates and three AMS ^{14}C samples were analyzed. One OSL sample (6024 ± 243 a BP) from 483 cm in the core is inverted and significantly older. Considering that it may have been affected by anthropogenic disturbance or lake erosion, it was not used to construct the chronological framework. After eliminating the outliers, the Age-depth was constructed based on the method of piecewise fitting. The established Age-depth model is shown in Fig. 3.

Characterization of geochemical elements

A comprehensive geochemical analysis of major oxides (MgO, Al_2O_3 , CaO, Na_2O , K_2O) and trace elements (Rb, Sr, Ti) in the profile samples has been conducted, with the results detailed in Table 3. It also details the minimum, maximum, mean, standard deviation (SD) and coefficient of variation (CV)

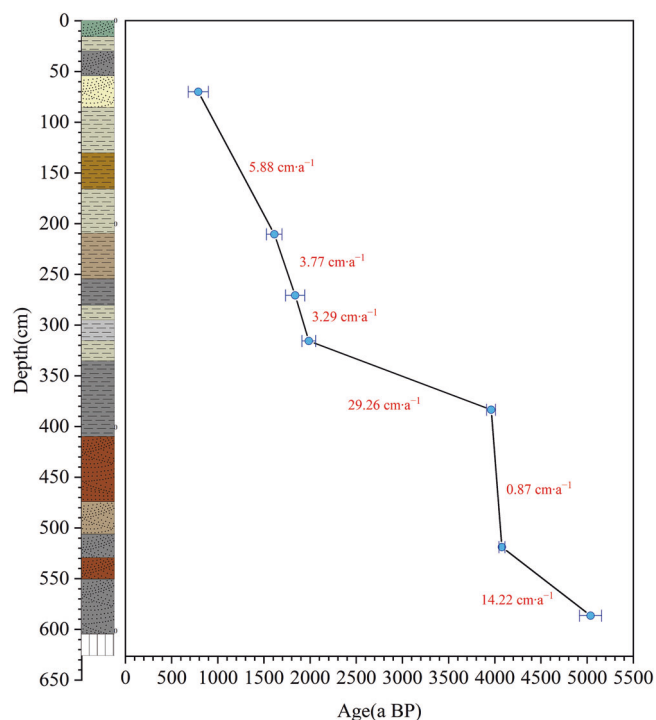


Fig. 3 | Age-depth model of the FHZ section. Age-depth relationship for the FHZ section, showing sedimentation rates ($cm a^{-1}$) at different depths.

of the various elements at each stage and their comparison with the upper continental crust (UCC)³⁶. The element distribution patterns and lithological variations in each stage provide crucial insights into the sedimentary environmental changes and hydrological dynamics recorded in the profile. Based on the distribution characteristics of these elements and changes in stratigraphic lithology, the profile has been divided into four stages (I, II, III, IV) for detailed discussion (Fig. 4).

Stage IV (625–550 cm, 5.6–4.5 a BP): Compared with the UCC values, the contents of MgO (1.4%), Al_2O_3 (13.8%) and CaO (1.2%) show significant depletion, and the CV is large, indicating the different characteristics of the major elements during chemical weathering and deposition in the supergene environment. The Ti content ($4868.8 \mu g/g$) was significantly enriched, with a decreasing trend from the bottom to the top. The mean value of Rb ($126.9 \mu g/g$) was higher than the UCC value and was also significantly enriched, while the mean value of Sr ($103 \mu g/g$) was lower than the UCC value and was significantly deficient. The contents of Rb and Sr showed opposite trends, with the peaks of Rb corresponding to the troughs of Sr. Changes in geochemical element content fluctuate considerably in Stage IV, and it can be observed that such changes are associated with shifts in sedimentary environments.

Stage III (550–410 cm, 4.5–4 ka BP): The mean values of Al_2O_3 (11.8%), CaO (1.6%), Na_2O (1%) show varying degrees of deficit compared to the UCC. The mean values of Rb ($126.9 \mu g/g$) and Ti ($4119 \mu g/g$) are higher than the UCC values and are enriched. The Sr ($117 \mu g/g$) shows a significant deficit. Overall, the variation of geochemical element content in stage III is relatively small, and the coefficient of variation is relatively small among the four stages. This indicates that the sedimentary environment at this time is relatively stable and there are relatively few sources of material.

Stage II (410–210 cm, 4–1.6 a BP): MgO (1.1%), Al_2O_3 (11.2%), CaO (1.2%), Na_2O (1.1%), K_2O (2.2%), Sr ($114.0 \mu g/g$) showed a significant deficit compared to the UCC values, while Rb ($114.5 \mu g/g$), Ti ($4481.9 \mu g/g$) were enriched. Rb, CaO, MgO showed a gradual decreasing trend from bottom to top, while Ti and Na_2O were the opposite. Among them, anomalously low values of Ti, Sr, Na_2O , K_2O , Al_2O_3 , and MgO appeared in the interval of 280–220 cm (1.9–1.6 ka BP). This may be due to the occurrence of anomalous climatic events that affected the hydrological state at this time, resulting in the migration of geochemical elements. The trend of most of the geochemical element contents during this stage showed drastic fluctuations, which may be related to changes in the sedimentary environment and intensification of human activities, resulting in unstable migration or enrichment of the elements.

Stage I (210–0 cm, 1.6 ka BP~present): After the anomalous deficit in Stage II, all the geochemical elements resumed a stable trend in Stage I. During 120–80 cm (1.1–0.8 ka BP), the contents of K_2O , MgO, and Al_2O_3 showed wave peaks and then began to decline again. However, in general, the magnitude of elemental changes became smaller and the coefficients of variation were low, which may be that the depositional environment changed back to a stable state.

Analysis of particle size parameters

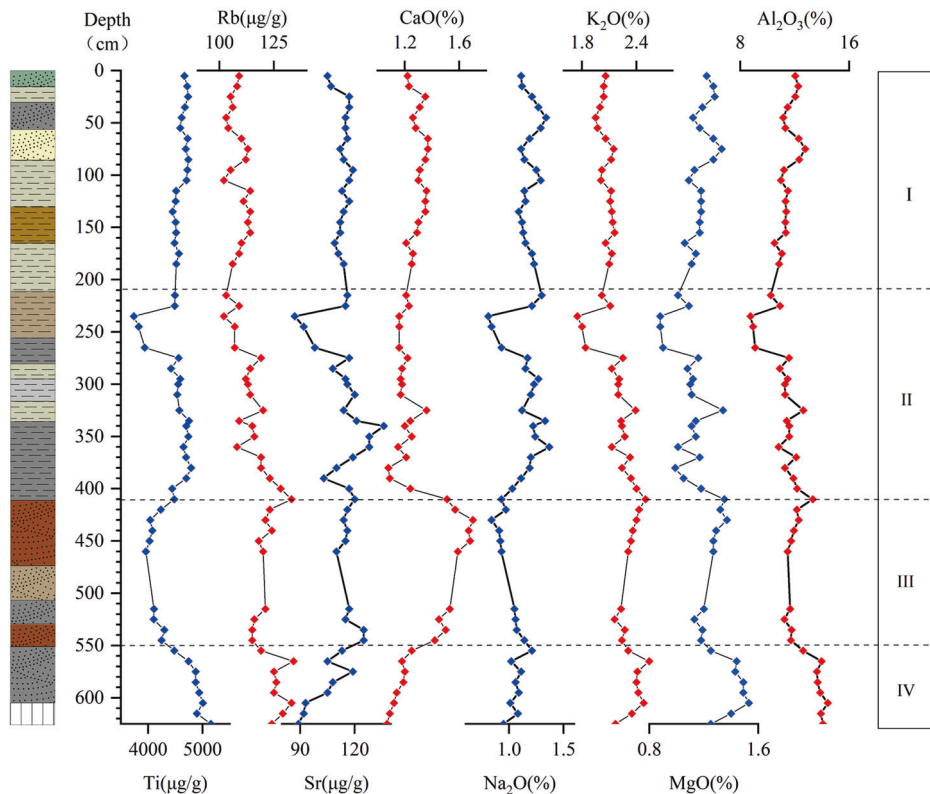
Based on the Folk and Ward grain size classification criteria³⁷, the sediments in the profile section were categorized into three grain size fractions: clay ($<3.9 \mu m$), silt ($3.9–62.5 \mu m$) and sand ($>62.5 \mu m$). In this study, several grain size parameter indices, such as median grain size (M_d), sorting (S_0), skewness (S_k), and kurtosis (KG), were used to reflect the grain size characteristics of the sediments. The results of the analysis of each particle size parameter are shown in Fig. 5, and the particle size variation of the whole profile can be divided into four stages:

Stage IV (625–550 cm, 5.6–4.5 ka BP): The raw soil layer (625–605 cm) consists mainly of silt (90.45%) and clay (8.52%). The M_d content ranges from 6.19–6.56 μm , with minimal particle size variation. The S_0 ranges from 1.46–1.57, indicating poor sorting, and S_k ranges from 0.19–0.3, suggesting coarse skewness. The KG ranges from 0.93–0.96, indicating medium KG. The stable M_z suggests a consistent source, but the S_0 and KG values indicate

Table 3 | The content of major elements and trace elements in FHZ section at each stage

		MgO(%)	Al ₂ O ₃ (%)	CaO(%)	Na ₂ O(%)	K ₂ O(%)	Rb(μg/g)	Sr(μg/g)	Ti(μg/g)
I	Min	1.1	10.5	1.2	1.1	2.0	102.0	105.0	4449.0
	Max	1.3	12.8	1.4	1.3	2.2	114.0	119.0	4736.0
	Mean	1.2	11.5	1.3	1.2	2.1	108.8	113.5	4611.6
	SD	0.1	0.6	0.1	0.1	0.1	3.9	3.5	99.1
	CV	5.9%	5.0%	3.9%	6.1%	3.0%	3.5%	3.1%	2.1%
II	Min	0.9	8.7	1.1	0.8	1.8	102.0	87.0	3739.0
	Max	1.4	13.3	1.5	1.4	2.5	133.0	136.0	4788.0
	Mean	1.1	11.2	1.2	1.1	2.2	114.5	114.0	4481.9
	SD	0.1	1.1	0.1	0.2	0.2	7.8	11.6	293.1
	CV	11.3%	10.3%	7.5%	13.4%	8.9%	6.8%	10.2%	6.5%
III	Min	1.1	11.2	1.4	0.8	2.2	115.0	110.0	3956.0
	Max	1.4	12.3	1.7	1.1	2.4	124.0	125.0	4298.0
	Mean	1.2	11.8	1.6	1.0	2.3	119.2	117.0	4119.2
	SD	0.1	0.3	0.1	0.1	0.1	3.2	4.7	108.2
	CV	5.8%	2.6%	6.1%	9.3%	3.6%	2.7%	4.0%	2.6%
IV	Min	1.3	12.6	1.1	1.0	2.2	119.0	89.0	4478.0
	Max	1.5	14.4	1.3	1.2	2.5	134.0	119.0	5153.0
	Mean	1.4	13.8	1.2	1.1	2.4	126.9	103.0	4868.8
	SD	0.1	0.5	0.1	0.1	0.1	4.6	10.0	185.0
	CV	7.1%	3.6%	4.9%	6.8%	4.4%	3.6%	9.7%	3.8%
	UCC	2.5	15.4	3.6	3.27	2.8	84	320	3950

Fig. 4 | Vertical distribution of geochemical elements in the FHZ section. Depth profiles of geochemical elements (Rb, CaO, K₂O, Al₂O₃, Ti, Sr, Na₂O, MgO) in the FHZ section, showing variations in concentration with depth.

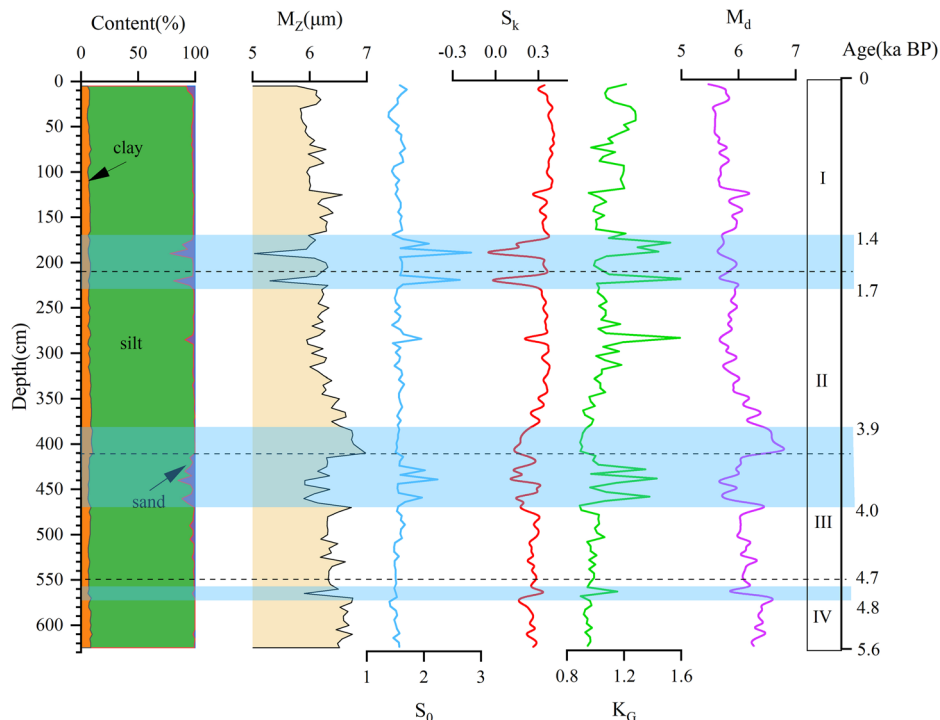


physical effects such as water erosion during deposition. The upper layer (605–550 cm, 5.3–4.5 ka BP) is mainly silt (91.75%) and clay (7.61%), with sand content dropping to 0.63%. The M_d ranges from 5.56–6.62 μm, indicating finer particles. The S_0 (1.39–1.53) shows poor sorting. S_K (0.15–0.39) is

mostly coarse (positive) and KG (0.89–1.15) is medium. These results suggest stable hydrodynamic conditions, typical of a lake or river environment.

Stage III (550–410 cm, 4.5–4 ka BP): This layer is primarily silt (89.36%) and clay (7.08%), with an increase in sand content (3.57%). The

Fig. 5 | Vertical distribution of particle size parameters in the FHZ profile. Depth profiles of particle size parameters (M_d , M_z , S_k , S_0 , K_G) and silt content in the FHZ profile. Blue shaded areas indicate periods of significant hydrological changes.



M_d ranges from 5.57–6.59 μm . The S_0 ranges from 1.47–2.24 indicating poor sorting. The S_k ranges from 0–0.38, mostly coarse (positive). The K_G ranges from 0.89–1.43, indicating medium kurtosis. These granulometric results suggest strong and stable hydrodynamic conditions, likely a river environment.

Stage II (410–210 cm, 4–1.6 ka BP): This layer is mainly silt (90.15%) and clay (7.9%), with sand content further increasing to 1.96%. The M_d ranges from 5.56–6.88 μm . The S_0 ranges from 1.44–2.63, indicating poor sorting. The S_k ranges from -0.17 –0.39, mostly coarse (positive). The K_G ranges from 0.89–1.63, indicating medium kurtosis. These results suggest a lake or river environment.

Stage I (210–0 cm, 1.6 ka BP–present): This layer is mainly silt (89.61%) and clay (8.93%), with sand content continuing to rise to 3.25%. The M_d ranges from 5.47–6.39 μm . The S_0 ranges from 1.38–2.89, indicating poor sorting. The S_k from -0.23 –0.42, mostly coarse (positive) and K_G ranges from 0.95–1.52, indicating narrow kurtosis. These results suggest significantly increased hydrodynamic conditions. The S_k supports this inference. The abnormal increase in sand content and poor sorting at 470–410 cm (4.0–3.98 ka BP) and 230–170 cm (1.7–1.4 ka BP) likely reflect local enhancements or changes in hydrodynamic conditions during deposition, possibly due to events like floods or storms. In the range of 410–380 cm (3.98–3.9 ka BP), the median and average particle size increased significantly, but the sand content decreased and the silt content increased significantly. This could be caused by rising water levels after a flood event.

Discussion

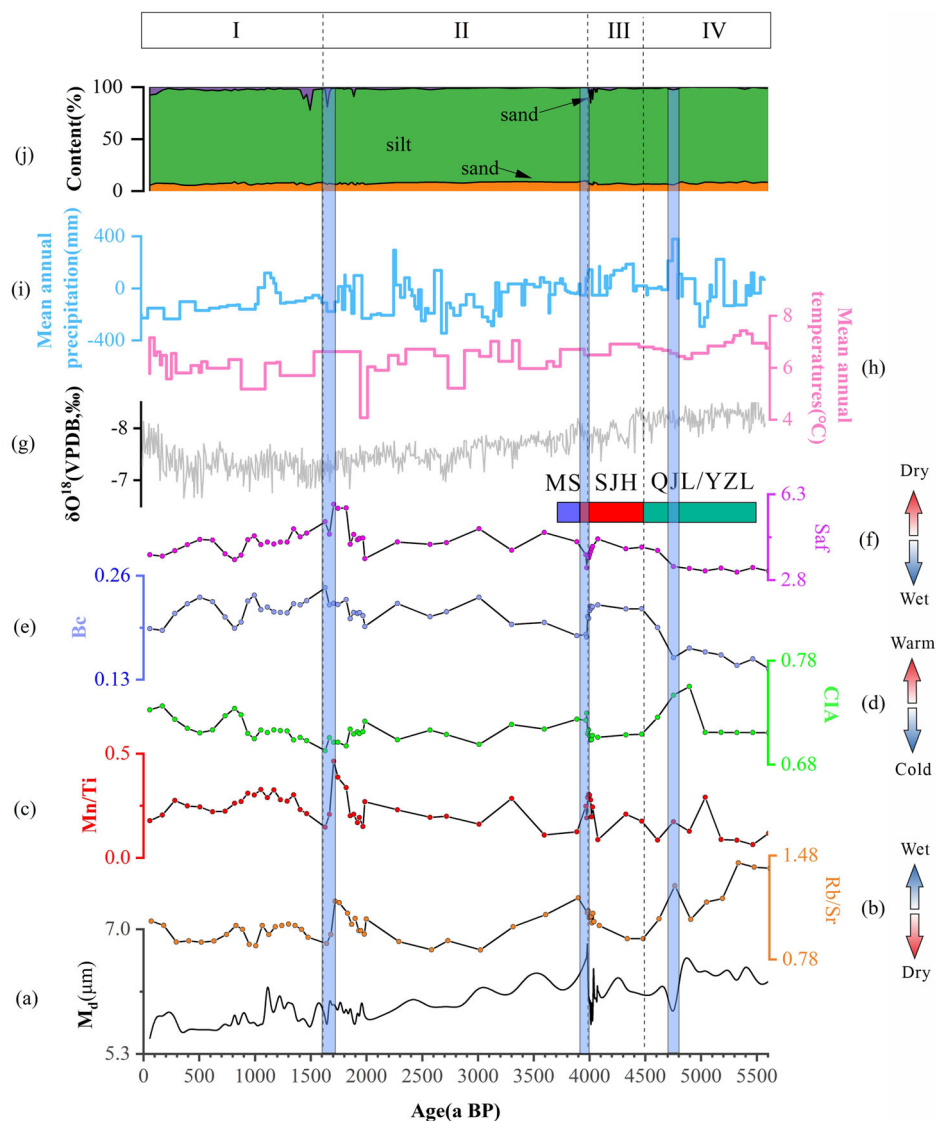
Holocene paleoclimate and sedimentary environment evolution

The sources, compositions, and content changes of geochemical elements in sediments are influenced by various factors, including watershed erosion, lake physicochemical processes, and the intrinsic geochemical behaviors of the elements during deposition³⁸. Understanding these factors is fundamental for reconstructing past depositional environment changes. The chemical index of alteration (CIA) is commonly used to reflect the degree of mineral alteration during weathering, an increase in CIA indicates enhanced chemical weathering. The determination of dealkalization coefficient (Bc) content is based on the degree of leaching of Na_2O and CaO from the sediment relative to Al_2O_3 , with lower values reflecting wetter depositional

environments. The secondary aluminum factor (Saf) is often used as an indicator of the degree of chemical weathering and climatic conditions of surface sediments and decreases with increasing weathering and warmth^{38–40}. The Rb/Sr ratio reveals stratigraphic depositional environments and palaeo-climatic variations, and higher Rb/Sr ratios usually refer to warmer and wetter climates because Rb is relatively stable, while Sr is susceptible to loss under heavy precipitation conditions^{38,41}. Conversely, lower Rb/Sr ratios indicate arid climates. Mn/Ti values are lower in reducing environments because Ti is relatively stable in depositional environments, whereas Mn dissolves in reducing environments, thus indicating changes in precipitation⁴¹. Analysis of elemental ratios from the FHZ section reveals that CIA is negatively correlated with Saf and Bc values, and positively correlated with Rb/Sr values (Fig. 6). Based on the elemental distribution characteristics and lithological changes, the paleoclimate changes at the FHZ site can be divided into four stages:

Stage IV (5.6–4.5 ka BP): The top of the raw soil layer is dated to about 5.3 ka BP, and it can be assumed that this moat was put into use during the early Qujialing culture (5.3–4.5 ka BP). Archaeological records show that the city wall was built during the Qujialing culture period. It shows that the moat and the wall should be built at the same time. The raw soil layer is dominated by silty clay, and the grain size characteristics indicate that this was originally a fluvial environment. The grains gradually became finer up to the upper layers, probably because it was after the construction of the moat that the hydrodynamics weakened. The CIA, Rb/Sr, and Mn/Ti values were overall high, and the Saf and Bc values were generally low. The combination of these data suggests that Stage IV was generally in a strongly weathered, warm and humid climatic environment. Among them, the values of CIA, Rb/Sr and Mn/Ti gradually increased during the period from 4.8–4.7 ka BP, reaching a peak at about 4.8 ka BP, while the Bc values appeared to have a trough, confirming that the FHZ site was in a strong weathering, warm and humid climate at this time. Sporulation records from the Yangtze River Valley also show a significant increase in rainfall during this period (Fig. 6i). This also corresponds to the stage of stronger summer winds in East Asia recorded by the $\delta^{18}\text{O}$ sequence of Donggedong cave stalagmite DA (Fig. 6g). During 4.8–4.7 ka BP, the grain size parameters also showed abnormal fluctuations, which may be caused by heavy precipitation in

Fig. 6 | Comparison of paleoclimate proxies form FHZ section. a Distribution of M_d values form FHZ section. **b–f** Climate proxies of FHZ section. CIA, Saf and Bc refer respectively to the chemical index of alteration, secondary aluminum factor and dealcalization coefficient. **g** $\delta^{18}O$ sequence of Dongge Cave stalagmite DA⁶⁸. **h** Mean annual temperatures of pollen reconstruction from Dajiuhe Lake in the Shennongjia peat profile⁶⁹. **i** Mean annual precipitation downstream of the Yangtze River based on pollen reconstruction⁷⁰. **j** Grain size fractions form FHZ section. The QJL, SJH, MS and YZL in the color band represent the Qujialing culture, the Shijiahe culture, the Meishan culture and the Youziling culture, respectively. The blue shaded area is the flooding period.



warm and humid climates. The flood event carried a large amount of fine-grained material and deposited in the river channel, resulting in a decrease in the median particle size. Floods may bring sediments from different sources, making the S_o , S_k and KG of sediments increase (Fig. 5). The content of medium-fine silt is prominent, and 10–40 μm accounts for a considerable share, which is consistent with the characteristics of multi-suspended silty sand in flood layer sediments⁴². During 5–4.5 ka BP, the climate of the Jiangnan Plain was particularly unstable, and the lakes were in a period of instability or continuous change⁴³. The two major flood events in the mid-late Qujialing culture (4.9–4.6 ka BP) and the late Shijiahe culture to the Xia Dynasty (4.1–3.8 ka BP) are common in the site strata of the Jiangnan Plain⁴⁴. However, from 4.7–4.5 ka BP, the CIA, Rb/Sr and Mn/Ti values gradually decreased to the valley value, and the Bc and Saf values began to rise to the peak value. This indicates that the weathering is weakened and the climate gradually turns dry and cold.

Stage III (550–410 cm, 4.5–4 ka BP): 4.5–4 ka BP, CIA, Rb/Sr continued to remain low, and the Saf and Bc trends were opposite. These indicators show a weakening of weathering, a decrease in rainfall, and a colder environment at this time. However, compared with stages II and I, the climate from 4.5–4.2 ka BP was warmer. The stalagmite record shows that the East Asian summer winds weakened during this period compared to the previous period (Fig. 6g). The climatic drought events around 4.2 ka BP that occurred during this period spread throughout the northern hemisphere at

low and mid-latitudes, and were an important cause of the decline of pre-historic civilizations and migration of peoples^{45,46}. Many large settlements in the Yangtze River basin, including the Shijiahe site, were abandoned⁴⁹. The function of the city wall at the FHZ site disappeared, the moat continued to be used as a ring trench, and the site changed from a central settlement to an ordinary settlement³⁰. A severe flood event was recorded at the FHZ site stratigraphy around 4–3.9 ka BP. The CIA, Rb/Sr, and Mn/Ti were anomalously elevated, corresponding to peaks in Saf and Bc values (Fig. 6). The M_d of the sediments is anomalously elevated after a decrease, and the sand content is significantly higher (Fig. 6a, j). This is consistent with the stratigraphic record of flooding during the Qujialing culture period mentioned above⁴⁴. A major flood event caused by climatic fluctuations around 4 ka BP may have accelerated the collapse of the Shijiahe culture⁴⁷.

Stage II (410–210 cm, 4–1.6 ka BP): During the period of 4–2.7 ka BP, CIA, Rb/Sr generally show a decreasing trend, while Saf and Bc values slightly increase. It indicates that weathering weakened and the climate continued to be dry and cool environment. Stalagmite records show a further weakening of monsoon action during this period (Fig. 6g). But the fluctuations in the elements indicate a very unstable climate at this time. At this time, the Meishan culture in northern China advanced southward to the Jiangnan Plain to replace the Shijiahe culture, forming the Meishan culture Xiaojiajaoji type⁴⁸. Until about 2.6 ka BP, the CIA, Rb/Sr started to rise, and the climate gradually changed to warm and humid. By 2–1.7 ka BP, the CIA,

Rb/Sr rose sharply and peaked, while the contents of Saf and Bc rose, but there was a trough. This shows that the depositional environment changed at this time, and it is speculated that this may be related to the southward migration of the Chu state⁴⁹. In the 1.7–1.6 ka BP, were again abnormally elevated, and the S₀ and sand content were also elevated again. This indicates that at this time, the Fenghuangzui site was again subjected to flooding. This corresponds to the paleoflood layer (1597 a BP) of the DongJin Dynasty in the sedimentary record of the Jiangling profile in the Jiangnan Plain⁵⁰.

Stage I (1.6 ka BP~present): The fluctuation of each environmental substitution index is pronounced. The overall environment of the Jiangnan Plain exhibits a trend towards increasing aridity, characterized by intensified erosion, rapidly changing water levels, and shifting sedimentary conditions. These changes are significantly influenced by human activities. However, during the period from 0.8–0.2 ka BP, there is a notable decline in the CIA and the Rb/Sr ratio (Fig. 6b, d), alongside a marked increase in Saf and Bc concentrations (Fig. 6e, f). This suggests a period of weak weathering and a cold, dry climate. Pollen records from this time also indicate a reduction in rainfall (Fig. 6i), which aligns roughly with the Little Ice Age during the Ming and Qing Dynasties (0.7–0.3 ka BP)⁵¹. Archaeological findings from

ceramics further support this, indicating that the moat continued to be used during these dynasties.

Multifactorial considerations in the site selection for FHZ settlement

The site selection of prehistoric human settlements depended on two primary factors: efficient and convenient use of natural resources and avoidance of natural or social risks⁵². These factors were closely related to climate, regional hydrologic environments, and topographic and geomorphic contexts. Around 5.5 ka BP, the water levels of rivers and lakes in the middle Yangtze River decreased, expanding the land available for human settlement. This facilitated the increase and aggregation of settlements⁵³. The fertile alluvial plains were suitable for rice agriculture, which eventually replaced hunting and gathering as the primary subsistence economy¹⁹. During the Qujialing-Shijiahe culture period (5.3–3.9 ka BP), early central settlements in the middle Yangtze River region acted as regional cultural center controlling surrounding settlements, forming a four-tier settlement hierarchy: super settlements, large and medium-sized settlements, small settlements, and ordinary settlements⁵⁴. The FHZ site, covering

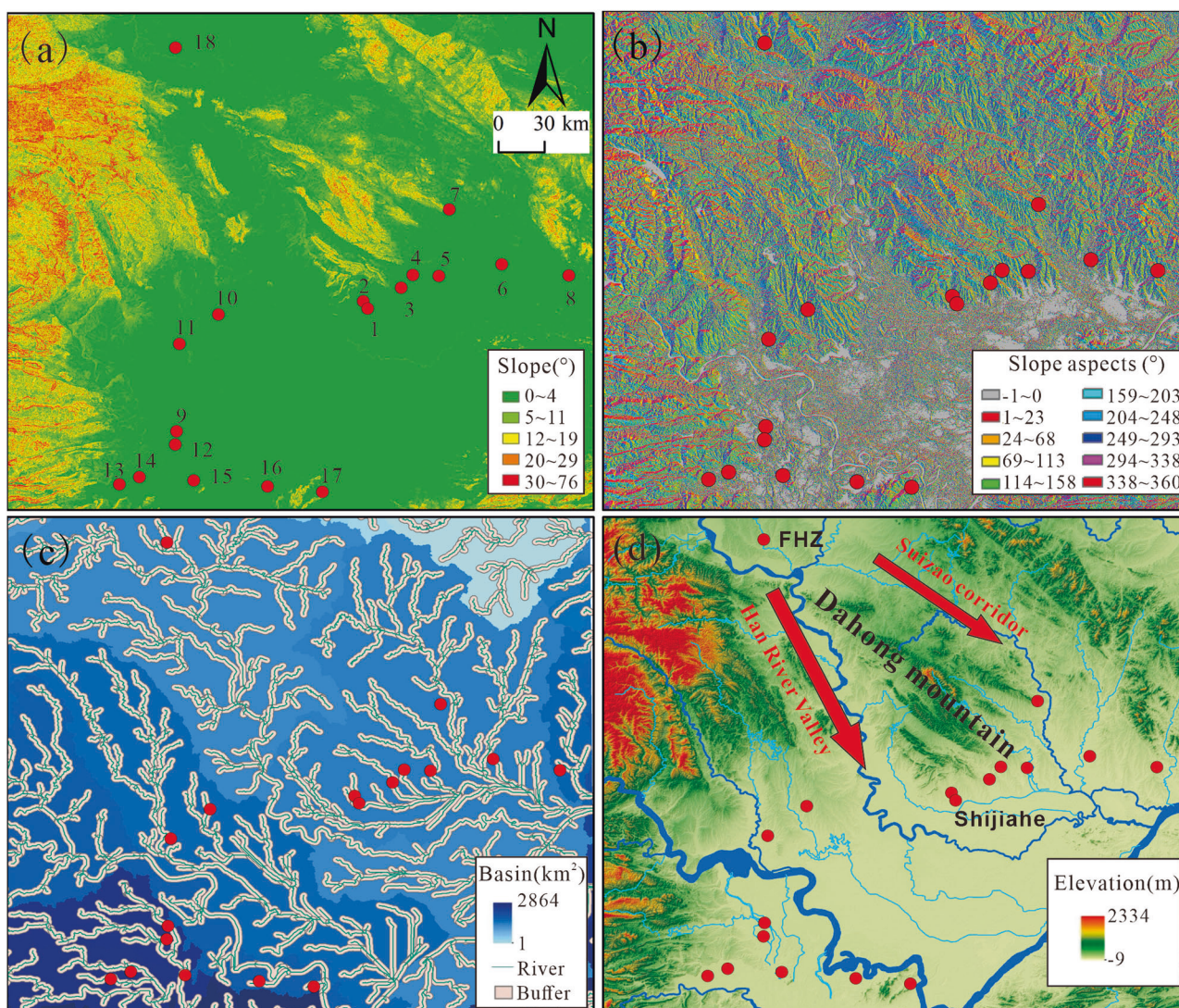


Fig. 7 | Hydrological and geomorphological analysis of central settlements in the middle Yangtze River region. a, b Spatial distribution of slope and aspect, highlighting the topographic characteristics of the central settlements. **c** River buffer zone (2 km) and basin analysis, illustrating the proximity of settlements to water resources. **d** Elevation extraction of central settlements, emphasizing the

relationship between settlement locations and terrain. The prehistoric central settlements are 1: Shijiahe, 2: Longzui, 3: Xiaocheng, 4: Taojiahu, 5: Menpanwan, 6: Yejiamia, 7: Wangguyao, 8: Zhangxiwan, 9: Chenghe, 10: Majiawan, 11: Yinxiangcheng, 12: Jimingcheng, 13: Chengtoushan, 14: Jijiaocheng, 15: Qinghe, 16: Zoumaling, 17: Qixingdun, 18: FHZ.

Table 4 | Analysis of topographical factors in prehistoric central settlements in the middle Yangtze River region

No	Site	Slope(°)	Aspect(°)	Elevation(m)	Basin(km ²)
1	Shijiahe	0.4	281.3	31	1001
2	Longzui	2.1	202.2	32	1001
3	Xiaocheng	0.5	81.9	28	1001
4	Taojiahu	1.2	280.0	48	1001
5	Menbanwan	0.2	71.6	29	1001
6	Yejiamao	0.4	90.0	29	1001
7	Wangguliu	0.6	104.0	63	1001
8	Zhangxiwan	0.4	31.0	30	1206
9	Chenghe	0.8	0.0	37	1720
10	Majiawan	1.0	8.1	59	1173
11	Yinxiangcheng	1.3	3.0	40	1173
12	Jimingcheng	0.6	14.0	39	1720
13	Chengtoushan	0.2	251.6	42	1725
14	Jijiaocheng	0.5	98.1	38	1725
15	Qinghe	0.7	71.6	36	1720
16	Zoumaling	1.0	118.3	32	1245
17	Qixingdun	1.6	285.3	55	1245
18	FHZ	0.4	198.4	88	932

approximately 140,000 m², is classified as a large and medium-sized settlement. To explore the relationship between the site selection of the FHZ settlement and its regional hydrologic geomorphology, we used Geographic Information System (GIS) technology to assess the distribution of water systems and topographic contexts. By combining this data with records from other central settlements, we inferred potential reasons for early human selection of this site. The analysis results of the slope and orientation of prehistoric cities in the middle Yangtze River, the buffer zone, and the basin area are presented in Fig. 7 and Table 4.

Topographically, with the exception of the Longzui site, all of the early cities had slopes of 2° or less (Fig. 7a, Table 4), suggesting that gentle topography was an important site selection factor. This is because gentle terrain not only facilitates crop cultivation and irrigation, but also reduces the difficulties of farming caused by undulating terrain. In central settlements such as Shijiahe settlement and Yinxiang settlement, large areas of low-lying land were found, in which drilling and analysis revealed a high content of rice siliceous bodies^{19,55,56}. These farming areas were 1–2 m lower than the settlement areas, close to rivers and lakes, and connected to the water system⁵⁶. Rice agriculture dominated the FHZ settlement, which has a slope of 0.4°, in line with the characteristics of the site selection of central settlements in the middle Yangtze River region. The results of aspect analysis show that there is no correlation between the orientations of the sites selected among the central settlements, which may be related to the location of the water system around each of them (Fig. 7b, Table 4). The FHZ settlement has a slope orientation of 198.4°, and its orientation belongs to the due south direction (159–203°). The moat of FHZ site flows eastward into a

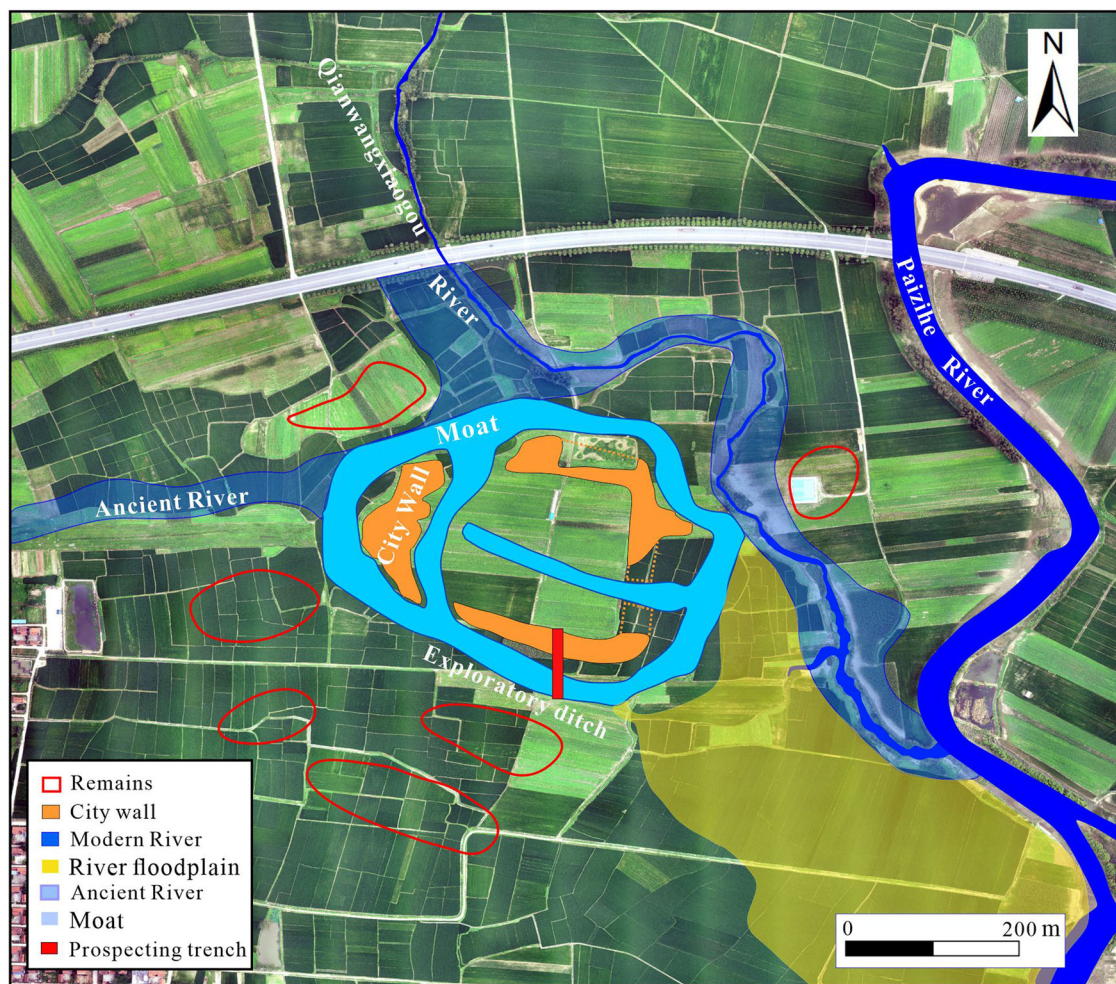


Fig. 8 | Landscape scheme of the FHZ site. Schematic of the FHZ site showing ancient and modern rivers, remains, city walls, and floodplains (Provided by the archaeological team of FHZ Site, Wuhan University).

northwest-southeast oriented ancient river channel (called Qianwangxiaogou river), and then southeastward into the Paizhe River, a tributary of the Hanjiang River (Fig. 8). According to archaeological records, there are many cultural remains and large areas of ancient floodplain deposits in the south of the FHZ site (Fig. 8). The southern orientation of the inner settlement greatly enhanced accessibility to subsidiary settlements, facilitating communication and exchange. Considering the geomorphological characteristics of the river floodplain, it is likely that this area included cultivation zones, warranting further investigation.

The hydrologic analysis reveals that nearly all sites are within a 2 km buffer zone of the water system. A stable water supply from sources such as rivers, lakes, or springs was crucial for meeting domestic needs and supporting agricultural irrigation (Fig. 7c). Additionally, proximity to rivers facilitated waterborne transport and trade, thereby promoting economic growth⁵⁷. Basin analysis, which delineates basins by identifying ridgelines, indicates that sites within the same basin are more accessible and connected. According to Table 4, basins measuring 1001 km² and below, as well as those 1720 km² and above, contain more settlements. These areas correspond to the regions south of the Dahong Mountains and the northwestern part of Dongting Lake, respectively, when considering modern water systems and landforms. The largest central settlement in these regions was Shijiahe settlement (1200,000 m²), followed by Chenghe settlement (600,000 m²)⁵⁴. These areas may have been key control zones for the Qujialing culture (Fig. 7c). The watershed containing the FHZ site borders that of the Shijiahe site, separated by the Dahong Mountain. As can be seen from Fig. 7c, d, the western basin of Dahongshan corresponds to the Hanjiang River valley, which used to be controlled by the Majiawan and Yinxiangcheng sites. The eastern basin corresponds to the Suizao corridor, which used to be controlled by the Yejiamiao, Wangjialiu, and Zhangxiwan sites. This geographical distribution complicates efforts to protect the Shijiahe site. Without the watershed controlled by the FHZ site, northern cultures could have potentially invaded the Shijiahe site from both sides of Dahong Mountain. Consequently, in the event of an invasion by northern cultures, the FHZ site could relay warnings to the Shijiahe site via the Han River system. The Nanyang basin has historically served as a significant corridor for cultural exchange between northern and southern China⁵⁸. The FHZ site played a pivotal role in facilitating the territorial expansion of the Qujialing-Shijiahe culture into the Nanyang Basin, situated at the confluence of the Jiangnan Plain and the Central Plains. The establishment of the FHZ site served as a strategic outpost for the Qujialing culture in its interactions and conflicts with northern cultures.

The study area was selected for urban construction due to its proximity to water sources and agricultural suitability. The FHZ settlement utilized the Qianwangxiaogou river to construct a moat, channeling water from the north to the Paizhe River. There are two ancient rivers about 20 m wide in the FHZ settlement in a “T” shape. One runs east-west, passing east through the middle of the east wall and connecting with the moat (Fig. 8). This system introduced reservoir water into the settlement via moats, forming an irrigation network that ensured a stable water supply, supported rice agriculture and handicrafts, and served multiple functions such as transportation, defense, flood control, and drainage. Rice farming, the economic foundation of the region, offered high production efficiency, providing high-quality food and sustaining a large population³¹. Various sizes of rammed earth mounds were found in the settlement, primarily distributed along the east-west riverbanks and in other areas, where the main use would have been for flood control. The main part of the settlement has an elevation of 88 m (Table 4), much higher than other sites. Around the wall length of about 170–280 m, width of 16–70 m, the overall higher than the outer lowland 1–2 m. The choice of electing higher ground helped mitigate flood risks, and natural river bends slowed water flow, reducing flooding threats. The FHZ settlement was situated on elevated terrains such as hills, offering strategic vantage points and enhancing defense capabilities. The fertile soil between the rivers ensured agricultural productivity, securing food supplies. In addition, the site may have been chosen with transport connectivity and defence needs in mind. The dense river network ensured the efficient movement of people and goods, while creating natural topographical obstacles to minimize external threats.

The mechanism driving the rise and decline of FHZ settlement

The sedimentary records from Miancheng core indicate that the most favorable climatic conditions in the Jiangnan Plain occurred between 6.8–4.9 ka BP. From 6.8 ka BP onwards, there was evidence of river flooding, and numerous lakes were present across the Jiangnan Plain during this period, which marked the precursor stage to the formation of Guyunmengze (Fig. 9b)⁵⁹. From the Daxi culture to the Youziling culture (6.5–5.3 ka BP), ancient cities with walls, moats, and irrigation facilities, such as Chengtoushan site and Longzi site, appeared in the Dongting Lake Basin and Jiangnan Plain, benefiting from superior hydrological conditions¹⁹. The Youziling culture (5.7–5.3 ka BP) emerged on the left bank of the Hanshui River and rapidly spread westward, covering the area previously influenced by the Daxi culture.

During 5.3–4.5 ka BP, the study area experienced a warm and humid climate with increased weathering, providing favorable hydrothermal conditions for rice cultivation (Fig. 6). A large number of carbonized rice seeds from the Qujialing period were unearthed at the FHZ site³². The Qujialing culture (5.3–4.5 ka BP), which developed from the Youziling culture, unified prehistoric cultures in the middle Yangtze River. This period saw significant societal transformations and a dramatic expansion of influence throughout the entire middle Yangtze River region. The Qujialing culture also exhibited a strong trend of expansion toward the central plains and maintained interactions with the Liangzhu culture in the lower Yangtze River region⁶⁰. During this time, the weakening of the summer monsoon led to decreased rainfall, compelling ancient societies to develop irrigation systems to meet agricultural and domestic needs. This necessity likely promoted the emergence of ancient central settlements and the development of complex social structures¹⁹. In addition, the frequent floods in the Jiangnan Plain also prompted the Qujialing culture to build a perfect water conservancy system to withstand floods (Fig. 9a). Sections from the Zhongqiao site in the Jiangnan Plain⁶¹ and the Sanfangwan site within the Shijiahe site⁴⁴, as well as the Wuhan natural depositional borehole ZK145⁶², record flooding events that probably occurred during the middle of the Qujialing culture (Fig. 9a, b). Prehistoric central settlements emerged in this period, such as Shijiahe site, Taojiahu site, Yinxiang site, Jimingchen site and other central settlements with walls and trenches, and appeared the embryonic form of central settlements and subordinate settlements⁶³. The Shijiahe settlement became the central settlement of the middle Yangtze River region, the social division of labor was refined, and there were large sacrificial places⁵⁴. The walls at the FHZ site were constructed during the early Qujialing culture period (around 5.3 ka BP), likely reflecting a strategic need to expand northward. As the northernmost Qujialing cultural site, the FHZ site served as a critical gateway between the Jiangnan Plain and northern regions. Archaeological evidence suggests that this area was the initial northern penetration point for the Qujialing culture from the Jiangnan region, where it eventually established dominance. The culture later expanded into southeastern Shaanxi, southern and central Henan, and southwestern Shanxi⁶⁰. The rise of the FHZ site is closely linked to the northward expansion of the Qujialing culture and frequent cultural interactions between the north and south. It was an important control point and possibly a military stronghold.

During 4.5–3.9 ka BP, the study area experienced a drier climate and further weakened weathering, but the early climate was still warm. The defensive function of the city wall at the FHZ site had disappeared, but the moat continued to serve as a ring trench, transforming the site from a central settlement to an ordinary settlement. Benefiting from the stable social environment and well-developed rice agriculture in the middle Yangtze River, the Qujialing culture was transformed into the Shijiahe culture and settlements gradually shifted from the terraces to the alluvial and lacustrine plains⁵⁸. It is highly probable that the climatic changes sweeping across Eurasia between 4.2–4 ka BP led to the collapse of ancient civilizations, including that of the Yangtze and Mesopotamian Plains^{19,64}. Almost all major prehistoric cities in the Yangtze River basin were abandoned around 4 ka BP, with many settlements suddenly disappearing⁵⁸. In addition, flood events were also a significant factor in the abandonment of the FHZ site. A major flood event that occurred at the end of the Shijiahe culture has also been discovered at the

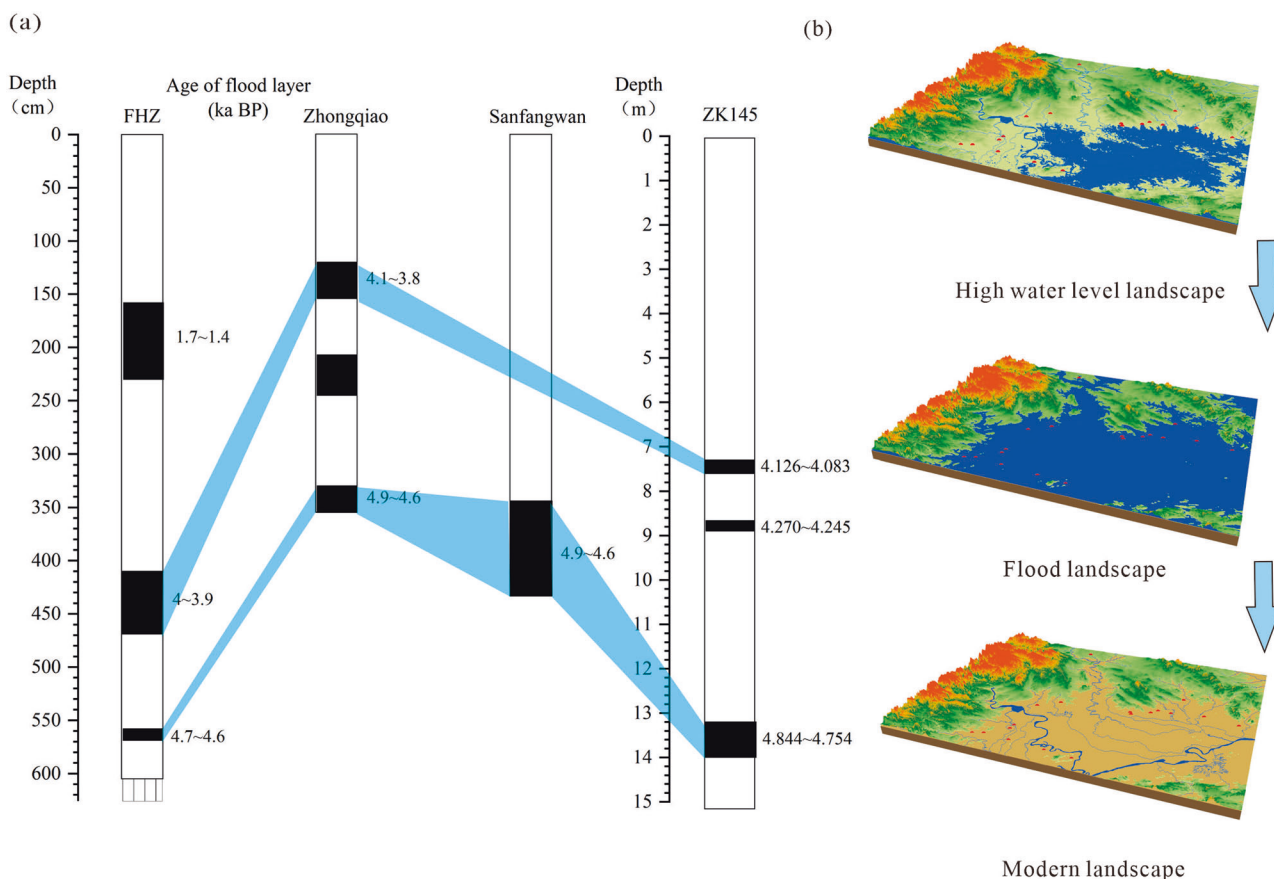


Fig. 9 | Flood layer correlation and landscape evolution in the middle Yangtze River. **a** Comparison of the flood layer from the archaeological sites^{42,61} and the ZK145 core in Wuhan⁶². **b** Landscape evolution sketch of the middle Yangtze River region.

Zhongqiao site and the Sanfangwan site^{42,61} (Fig. 9a). The flood event at the FHZ site in the Nanyang Basin corresponds roughly to the timing of the flood event recorded at the Jiangnan Plain site as well as the Wuhan core⁶². However, the occurrence of flooding at the FHZ site was relatively short, which may be related to the high topography. The shift in the function of the FHZ settlement during the Late Shijiahe culture period may have been due to the deposition of floodwaters that raised the moat and rendered the walls defenseless. The moat only had the function of irrigation left, and the FHZ settlement transformed into a weakly defended ring-trench settlement.

After the Shijiahe culture, the FHZ site was occupied by the Meishan culture from the Central Plains (3.9–3.7 ka BP) before being entirely abandoned. The Shijiahe culture is often associated with the Sanmiao cultural settlement, and the Sanmiao cultural settlement and the northern Central Plains cultural settlement often have large-scale conflicts and wars⁶⁵. According to historical records, Yu, the leader of the Central Plains cultural settlement, attacked the Sanmiao cultural settlement when the middle reaches of the Yangtze River was hit by natural disasters such as heavy rains and earthquakes⁴³. Evidence of cultural conflict has also been found in the Gujiapo cemetery near the FHZ site, with a large number of unearthened human bones and weapons showing the intensity of the war⁶⁶. We hypothesize that after the walls of the FHZ site were rendered useless, the Xia culture in the north took advantage of the opportunity to invade. The Shijiahe site, which is at a lower elevation than the FHZ site, was also caught in a flood disaster at this time, and the Xia culture was able to defeat the Sanmiao culture. The FHZ site lost its role as an outpost of the Shijiahe culture, so the Meishan culture was abandoned by the Xia culture at the transfer center afterward. At about 1.7–1.6 ka BP it was relatively dry (Fig. 9b), and with the discharge of the Dongjing River and Hanjiang River, the Jiangnan Plain quickly dried up to land. At about 1.7 ka BP, the lake stabilizes and forms an alluvial plain⁵⁹.

Conclusions

This research reconstructs the geomorphological, hydrological, and climatic conditions of the regional environment surrounding the FHZ settlement through detailed analysis of stratigraphic lithology, grain size parameters, and elemental geochemical records extracted from sedimentary sequences in the southern moat. These records provide a comprehensive reflection of climate variability, hydrological changes, and their implications for the cultural development history of the site during the mid-late Holocene.

The stratigraphic profile of the FHZ settlement provides a detailed record of environmental changes in the region since the mid-late Holocene. Between 5.6–4.5 ka BP, elevated CIA, Rb/Sr, and Mn/Ti values suggest a warm and humid climate conducive to intense weathering. A notable increase in grain size parameters around 4.8–4.7 ka BP indicates a flood event likely triggered by heavy rainfall. From 4.5–3.9 ka BP, declining CIA and Rb/Sr values alongside rising Saf and Bc values indicate reduced weathering and a shift towards a cooler, drier climate. Another significant flood event occurred between 4–3.9 ka BP. During 3.9–2.7 ka BP, further declines in CIA and Rb/Sr values and slight increases in Saf and Bc values suggest sustained dry and cool conditions with diminished weathering. Between 2.7–1.6 ka BP, rising CIA and Rb/Sr values indicate a transition to a warmer and more humid climate. Around 1.7–1.6 ka BP, another flood event occurred. From 1.6 ka BP to the present, climatic proxies show significant fluctuations. Notably, during 0.8–0.2 ka BP, sharp declines in CIA and Rb/Sr values alongside abnormal increases in Bc and Saf values reflect the peak of the Little Ice Age during the Ming and Qing dynasties, marked by a significant temperature drop.

The location of the FHZ settlement has a complex relationship with its geomorphology and hydrological environment. Early settlers strategically placed the walls on high ground and built moats to connect them to natural waterways. The river network is both a natural barrier and an important water source for rice cultivation. The design of the inner settlement, which

faces directly south, takes into account the water system and agricultural areas. The purpose of Qujialing cultural settlement establishing FHZ settlement on the east bank of Han River is to expand its influence and protect the nearby Shijiahe settlement.

The FHZ settlement was built in the early period of Qujialing culture (5.3 ka BP) to resist the northern culture and protect Shijiahe settlement. The warm and humid climate is conducive to agricultural activities, contributing to the prosperity of the FHZ settlement. However, by the late Shijiahe culture (4–3.9 ka BP), the decrease of precipitation and temperature led to the decline of Shijiahe culture in the middle Yangtze River. Flooding events during this period rendered the FHZ walls defenseless. Subsequently, the FHZ settlement was invaded and eventually abandoned by the Meishan culture from the Central Plains. This refined analysis highlights the dynamic interplay between environmental factors and human settlement strategies in the FHZ settlement, providing insights into its rise, adaptation, and eventual decline during the Holocene.

Data availability

No datasets were generated or analysed during the current study.

Received: 12 July 2024; Accepted: 21 November 2024;

Published online: 07 February 2025

References

1. Roberts, N. et al. Human responses and non-responses to climatic variations during the last Glacial–Interglacial transition in the eastern Mediterranean. *Quat. Sci. Rev.* **184**, 47–67 (2018).
2. Panin, A. & Matlakhova, E. Fluvial chronology in the East European Plain over the last 20 ka and its palaeohydrological implications. *CATENA* **130**, 46–61 (2015).
3. Xiao, X. et al. Quantitative pollen-based paleoclimate reconstructions for the past 18.5 ka in southwestern Yunnan Province, China. *Glob. Planet. Change* **230**, 104288 (2023).
4. Kumar, V. et al. Bronze and Iron Age population movements underlie Xinjiang population History. *Science* **376**, 62–69 (2022).
5. Xu, D. et al. Synchronous 500-year oscillations of monsoon climate and human activity in Northeast Asia. *Nat. Commun.* **10**, 1–10 (2019).
6. Ardenghi, N. et al. A Holocene history of climate, fire, landscape evolution, and human activity in northeastern Iceland. *Climate* **20**, 1087–1123 (2024).
7. Blaus, A., Nascimento, M., Peterson, L., McMichael, C. & Bush, M. Climate, vegetation, and fire, during the last deglaciation in northwestern Amazonia. *Quat. Sci. Rev.* **332**, 108662 (2024).
8. Fan, D. et al. South flank of the Yangtze Delta: past, present, and future. *Mar. Geol.* **392**, 78–93 (2017).
9. Méndez C., Nuevo-Delaunay A., Reyes O., Belmar C., Mena F. Early Holocene Archaeological Context and Assemblages of Baño Nuevo 1: A Key Site in Central West Patagonia. *PaleoAmerica*, 2024; 1–18. <https://doi.org/10.1080/20555563.2024.2327129>.
10. Geirsdóttir, Á., Miller, G., Larsen, D. & Ólafsdóttir, S. Abrupt Holocene climate transitions in the northern North Atlantic region recorded by synchronized lacustrine records in Iceland. *Quat. Sci. Rev.* **70**, 48–62 (2013).
11. Kaniewski, D., Marriner, N., Cheddadi, R., Guiot, J. & Van, C. The 4.2 ka BP event in the Levant. *Climate* **14**, 1529–1542 (2018).
12. Sun, Q. et al. Climate as a factor for Neolithic cultural collapses approximately 4000 years BP in China. *Earth–Sci. Rev.* **197**, 102915 (2019).
13. Giosan, L. et al. Fluvial landscapes of the Harappan civilization, *Proceedings of the National Academy of Sciences*, 2012; 109, <https://doi.org/10.1073/pnas.1112743109>.
14. Huan, X. et al. Spatial and temporal pattern of rice domestication during the early Holocene in the lower Yangtze region China. *Holocene* **31**, 1366–1375 (2021).
15. Naudinot, N. & Kelly, R. Climate change and archaeology. *Quat. Int.* **428**, 1–2 (2017).
16. Mousa, F., El-Hassan, M. & Sallam, E. Terminal Holocene palaeolake mud pans (playas) of Farafra Oasis, Western Desert, Egypt: palaeoenvironmental and palaeoclimatic implications. *Int. J. Earth Sci.* **113**, 657–660 (2024).
17. Ru, T. et al. Mainstream migration events of the Yellow River and anthropogenic responses during the Mid–Holocene. *Quat. Int.* **685**, 14–23 (2024).
18. Du, T. et al. Sedimentary evidence for the diversion of the Yellow River onto the North China Plain 3000–2600 years ago. *Palaeogeogr., Palaeoclimatol., Palaeoecol.* **634**, 111909 (2024).
19. Yasuda, Y. et al. Environmental archaeology at the Chengtoushan site, Hunan Province, China, and implications for environmental change and the rise and fall of the Yangtze River civilization. *Quat. Int.* **123–125**, 149–158 (2004).
20. Sun, A. et al. Southward retreat of the Keriya River drove human migration in the Taklimakan Desert during the late Holocene. *Quat. Sci. Rev.* **332**, 108665 (2024).
21. Wang, C., Lu, H., Zhang, J., Gu, Z. & He, K. Prehistoric demographic fluctuations in China inferred from radiocarbon data and their linkage with climate change over the past 50,000 years. *Quat. Sci. Rev.* **98**, 45–59 (2014).
22. Li, B. et al. Linking the vicissitude of Neolithic cities with mid–Holocene environment and climate changes in the middle Yangtze River, China. *Quat. Int.* **321**, 22–28 (2014).
23. Liu J. Prehistoric Water Control Civilization in the Jiangnan Plain. Beijing: China Social Sciences Press, 2023. (in Chinese).
24. Chen Dongfang. Development of moats and the origin of cities. *Cultural Relics of Central China*, 2015: 42–45. (in Chinese).
25. Wu, L., Li, F., Zhu, C., Li, L. & Li, B. Holocene environmental change and archaeology, Yangtze River Valley, China: Review and prospects. *Geosci. Front.* **3**, 875–892 (2012).
26. Li, B. et al. Relationship between environmental change and human activities in the period of the Shijiahe culture, Tanjialing site, Jiangnan plain, China. *Quat. Int.* **308**, 45–52 (2013).
27. Li, J., Wang, S. & Mo, D. Environmental changes and relationship with human activities of Dongtinghu plain since 6000 a BP. *Acta Scientiarum Naturalium Universitatis Pekinensis* **47**, 1041–1048 (2011). (in Chinese).
28. Xia, Z. et al. Accurating dating of D/O events during 95–56 ka BP in East Asian monsoon: A case study of stalagmites from Shanbao cave, Shennongjia, China. *Sci. Sin. (Terra.)* **36**, 830–837 (2006). (in Chinese).
29. Deng, H., Chen, Y., Jia, J., Mo, D. & Zhou, K. Distribution patterns of the ancient cultural sites in the middle reaches of Yangtze River since 8500 a BP. *Acta Geographica Sin.* **64**, 1113–1125 (2009). (in Chinese).
30. Li Z., Wu T., Tian H. The Neolithic Site of Fenghuangzui, Xiangyang, Hubei. *Popular Archaeology*, 2021: 12–15. (in Chinese).
31. Lou, W. *Analysis of starch granules from stone artifacts excavated from the Fenghuangzui site, Xiangyang, Hubei Province.*, (2023). Wuhan: Wuhan University (in Chinese).
32. Huang X. Plant Macro-remains Unearthed from the 2020 Excavation at the Site of Fenghuangzui in Xiangyang. Wuhan: Wuhan University, 2023. (in Chinese).
33. Shi Z. Henan natural conditions and natural resources, Hena: Henan Science and Technology Press, 1983. (in Chinese).
34. Reimer, P. J. et al. The IntCal20 Northern Hemisphere Radiocarbon Age Calibration Curve (0–55 cal kBP). *Radiocarbon* **62**, 725–757 (2020).
35. Heaton, T. J. et al. The IntCal20 approach to radiocarbon calibration curve construction: A new methodology using Bayesian Splines and errors-in-variables. *Radiocarbon* **62**, 821–863 (2020).
36. Rudnick R. L., Gao S. Composition of the Continental Crust. In *Treatise on Geochemistry* (pp. 1–51). Elsevier, 2014. <https://doi.org/10.1016/b978-0-08-095975-7.00301-6>.

37. Folk, R. L. & Ward, W. C. Brazos River bar: a study in the significance of grain size parameters. *J. Sediment. Res.* **27**, 3–26 (1957).
38. Perri, F. Chemical weathering of crystalline rocks in contrasting climatic conditions using geochemical proxies: An overview. *Palaeogeogr., Palaeoclimatol., Palaeoecol.* **556**, 109873 (2020).
39. Wang, P. et al. The chemical index of alteration (CIA) as a proxy for climate change during glacial-interglacial transitions in Earth history. *Earth-Sci. Rev.* **201**, 103032 (2020).
40. Chen, C. et al. Variation of chemical index of alteration (CIA) in the Ediacaran Doushantuo Formation and its environmental implications. *Precambrian Res.* **347**, 105829 (2020).
41. Chang, H. et al. A Rb/Sr record of the weathering response to environmental changes in westerly winds across the Tarim Basin in the late Miocene to the early Pleistocene. *Palaeogeogr., Palaeoclimatol., Palaeoecol.* **386**, 364–373 (2013).
42. Wu, L. et al. Prehistoric flood events recorded at the Zhongqiao Neolithic Site in the Jiangnan Plain, Central China. *Acta Geographica Sin.* **70**, 1149–1164 (2015). (in Chinese).
43. Shi, C., Mo, D., Liu, H. & Mao, L. Late Neolithic cultural evolution and environmental changes in the northern Jiangnan Plain east of the Hanjiang River. *Quat. Sci.* **30**, 335–343 (2010). (in Chinese).
44. Wu L. Environmental Archaeological of the Mid–Holocene Palaeoflood in the Jiangnan Plain Central China, Nanjing: Nanjing University, 2013. (in Chinese).
45. Kerr, P. J. et al. Timing, provenance, and implications of two MIS 3 advances of the Laurentide Ice Sheet into the Upper Mississippi River Basin, USA. *Quat. Sci. Rev.* **261**, 106926 (2021).
46. Sionneau, T., Bout-Roumazeilles, V., Biscaye, P. E., Van Vliet-Lanoe, B. & Bory, A. Clay mineral distributions in and around the Mississippi River watershed and Northern Gulf of Mexico: sources and transport patterns. *Quat. Sci. Rev.* **27**, 1740–1751 (2008).
47. Guo L. Initial social complexity in the middle reaches of the Yangtze River (4300B, C, ~2000B, C.), Shanghai: Shanghai Ancient Books Publishing House, 2005. (in Chinese).
48. Yuan, F. *Research on Meishan Culture*, (2020). Wuhan: Wuhan University (in Chinese).
49. Zhu, C., Zhong, Y., Zheng, C., Ma, C. & Li, L. Relationship of archaeological sites distribution and environment from the Paleolithic Age to the warring states time in Hubei Province. *Acta Geographica Sin.* **62**, 227–242 (2007). (in Chinese).
50. Xie Y., Li C., Wang Q., Yin H. Sedimentary records of paleoflood events during the last 3000 years in Jiangnan plain. *Acta Geographica Sinica*. 2007:81–84. (in Chinese).
51. Tao, L., Su, J. & Kang, Y. *Reconstruction Anal. Chronol. high. Temp. events East. China Ming Qing dynasties.* **23**, 449–460 (2021). (in Chinese).
52. Li, Z., Zhu, C., Wu, G., Zheng, C. & Zhang, P. Spatial pattern and temporal trend of prehistoric human sites and its driving factors in Henan Province, Central China. *J. Geographical Sci.* **25**, 1109–1121 (2015).
53. Zhao, C. & Mo, D. Holocene hydro-environmental evolution and its impacts on human activities in Jiangnan–Dongting Basin, middle reaches of the Yangtze River, China. *Acta Geographica Sin.* **75**, 529–543 (2020). (in Chinese).
54. Liu H. The Settlement Structure and Social Form of Pre-Historic Cities in the Middle Reaches of the Yangzi River. *Jiangnan Archaeology*, 2017: 41–51. (in Chinese).
55. Nasu, H., Momohara, A., Yasuda, Y. & He, J. The occurrence and identification of *Setaria italica* (L.) P. Beauv. (foxtail millet) grains from the Chengtoushan site (ca. 5800 cal B.P.) in central China, with reference to the domestication centre in Asia. *Vegetation Hist. Archaeobotany* **16**, 481–494 (2006).
56. Da H. The research on the relationship between culture and ecological environment of Neolithic Age in the middle reaches of Yangtze River. Hubei: Central China Normal University, 2009. (in Chinese).
57. Macklin, M. G. & Lewin, J. The rivers of civilization. *Quat. Sci. Rev.* **114**, 228–244 (2015).
58. Deng, Z. et al. From Early Domesticated Rice of the Middle Yangtze Basin to Millet, Rice and Wheat Agriculture: Archaeobotanical Macro-Remains from Baligang, Nanyang Basin, Central China (6700–500 BC). *PLOS ONE* **10**, e0139885 (2015).
59. Zhu Y., Xue B., Yang X., Xia W., Wang S. Characteristic features of the sedimentary samples from the borehole M1 in Jiangnan plain and reconstruction of paleoenvironment. *Journal of Geomechanics*. 1997; 79–81+83–86. (in Chinese).
60. Shan S. A study on Qujialing culture, Wuhan: Wuhan University, 2019. (in Chinese).
61. Wu, L. et al. Mid–Holocene palaeoflood events recorded at the Zhongqiao Neolithic cultural site in the Jiangnan Plain middle Yangtze River Valley, China. *Quat. Sci. Rev.* **173**, 145–160 (2017).
62. Zhu, H., Zhang, Y. & Li, C. The application of end-member analysis in identification of paleo-floods in Wuhan section of the Yangtze River. *Acta Sedimentologica Sin.* **38**, 297–305 (2020). (in Chinese).
63. Wang H. The origin and function of moat settlement in the middle reaches of Yangtze River from the view of moat settlement in Menbanwan, *Archaeology*, 2003: 61–75. (in Chinese)
64. Kajita, H. et al. Extraordinary cold episodes during the mid–Holocene in the Yangtze delta: Interruption of the earliest rice cultivating civilization. *Quat. Sci. Rev.* **201**, 418–428 (2018).
65. Liu B. Discussion on Sanmiao and Sanmiao Culture. *Jiangnan Archaeology*, 2003; 30–32. (in Chinese).
66. Jia H. On prehistoric intertribal conflicts in multi-culture areas in light of the excavation of the Gujiapo Cemetery. 2004:77–86+96. (in Chinese).
67. Li, T. et al Surface treatment of red painted and slipped wares in the middle Yangtze River valley of Late Neolithic China: multi-analytical case analysis. *Heritage Science*, 2022; 10. <https://doi.org/10.1186/s40494-022-00824-0>.
68. Wang, Y. et al. The Holocene Asian Monsoon: Links to Solar Changes and North Atlantic Climate. *Science* **308**, 854–857 (2005).
69. Zhu, C. et al. Spore-pollen-climate factor transfer function and paleoenvironment reconstruction in Dajiuhu, Shennongjia, Central China. *Sci. Bull.* **53**, 42–49 (2008).
70. Li, J. et al. Quantitative Holocene climatic reconstructions for the lower Yangtze region of China. *Clim. Dyn.* **50**, 1101–1113 (2018).

Acknowledgements

This research was supported by Major Project of National Social Science Foundation of China: “Arrangement and Research on Archaeological Data of Zoumaling Prehistoric City Site” (19ZDA231).

Author contributions

Guo.A. : conceptualization, methodology, formal analysis, investigation, writing—original draft, writing—review and editing. Mao.L.: investigation, resources, supervision, funding acquisition. Li.C.: investigation.Mo.D. : validation, investigation, methodology, resources, supervision. All authors reviewed the manuscript.

Competing interests

The authors declare no competing interests.

Additional information

Correspondence and requests for materials should be addressed to Longjiang Mao.

Reprints and permissions information is available at <http://www.nature.com/reprints>

Publisher’s note Springer Nature remains neutral with regard to jurisdictional claims in published maps and institutional affiliations.

Open Access This article is licensed under a Creative Commons Attribution-NonCommercial-NoDerivatives 4.0 International License, which permits any non-commercial use, sharing, distribution and reproduction in any medium or format, as long as you give appropriate credit to the original author(s) and the source, provide a link to the Creative Commons licence, and indicate if you modified the licensed material. You do not have permission under this licence to share adapted material derived from this article or parts of it. The images or other third party material in this article are included in the article's Creative Commons licence, unless indicated otherwise in a credit line to the material. If material is not included in the article's Creative Commons licence and your intended use is not permitted by statutory regulation or exceeds the permitted use, you will need to obtain permission directly from the copyright holder. To view a copy of this licence, visit <http://creativecommons.org/licenses/by-nc-nd/4.0/>.

© The Author(s) 2025